Spectrochimica Acta Part A: Molecular and Biomolecular Spectroscopy 246 (2021) 118959

Contents lists available at ScienceDirect

Spectrochimica Acta Part A: Molecular and Biomolecular Spectroscopy

journal homepage: www.elsevier.com/locate/saa

A novel ratiometric fluorescent probe for selective detection and imaging of H_2S

Linlin Lv, Weiwei Luo, Quanping Diao *

School of Chemistry and Life Science, Anshan Normal University, Ping'an Street 43, Anshan 114005, China

ARTICLE INFO

Article history:
Received 30 July 2020
Received in revised form 12 September 2020
Accepted 13 September 2020
Available online 18 September 2020

Keywords:
H_2S detection
Fluorescent probe
Ratiometric
Cell imaging

ABSTRACT

In this work, a novel phenoxazine-based fluorescent probe **BPO-N_3** was developed to detect H_2S. The results showed that the probe had high selectivity and sensitivity toward H_2S, and its detection mechanism was based the ratio between green and red fluorescence signals; its detection limit was as low as 30 nM. The fluorescent imaging experiments further showed that the probe **BPO-N_3** could successfully detect endogenous and exogenous H_2S in living cells. This probe can be used as a powerful tool for in-depth study of H_2S function in various physiological processes.

1. Introduction

H_2S is a colorless, highly toxic, acidic gas with a smell of rotten egg. Recent studies have found that H_2S is the third gaseous signal molecule after NO and CO [1]. It is widely found in the human body and other organisms, and plays an important role in various physiological processes, such as regulating cell growth, protecting the cardiovascular system, taking part in anti-oxidation [2–5]. Therefore, the development of a simple and sensitive method for H_2S detection in living organisms is of great significance for further understanding of the physiological function of H_2S.

In recent years, the development of fluorescent probes that have high selectivity and sensitivity and can be used in living organisms has become a hot research topic [6–8]. Fluorescent probes are known to have high spatial and temporal resolution, thus can be used in real-time imaging by a fluorescent confocal microscope [9,10]. Although some excellent H_2S fluorescent probes with "off-on" or "turn-on" response have been reported [11–22], these probes have some limitations when they are employed in quantitative analysis as they are concentration-dependent and can be affected by test environments, excitation intensity and other factors. These factors can, however, be effectively eliminated by using the ratio fluorescent probe, by which the ratio of fluorescence intensity of two wavelengths is adopted in the quantitative analysis [23]. In addition, water solubility, light stability, emission wavelength, *etc.* can also restrict its application *in vivo* to a certain extent [24–26]. Therefore, it is still necessary to develop a ratio-type fluorescent probe that has good stability, high quantum yield, and long analytical wavelength. In this work, we designed a novel probe **BPO-N_3** using phenoxazine as the fluorescent matrix. We introduced an azide group, which is an electron-withdrawing group, into the phenoxazine matrix. Since the azide group can be effectively reduced to an amino group by H_2S [27–31], this electron-withdrawing group can be converted into an electron donor group on the phenoxazine fluorescent framework, which can then lead to the change of fluorescence spectrum. This mechanism can provide us with a ratio-type tool that can be used for detecting H_2S *in vivo*.

2. Experimental section

2.1. Instrumentation and reagents

UV–Vis and Fluorescence spectra were recorded on an F-2700 fluorescence spectrometer (Hitachi Co., Ltd. Japan) and Cary 50 UV–vis spectrometer (Varian Inc., USA) with a 1-cm quartz cuvette. ^1H NMR spectra were recorded on Mercury 300 BB NMR spectrometer (Varian Inc., USA). Mass spectra (MS) were performed on a Bruker microTOF Q II (Bruker Daltonics Inc., Germany). pH was measured on an INESA Scientific PHS-3C pH meter (Sartorius AG, Germany). Cell imaging experiments were carried out on an LSM 710 laser scanning confocal microscope (Carl Zeiss AG, Germany). All reagents were of analytical reagent grade and used without further purification or treatment. HepG2 (Human hepatocellular carcinomas) cells were obtained from the Anshan Central Hospital (Anshan, China).

* Corresponding author.
E-mail address: quanpingdiao@163.com (Q. Diao).

https://doi.org/10.1016/j.saa.2020.118959
1386-1425/

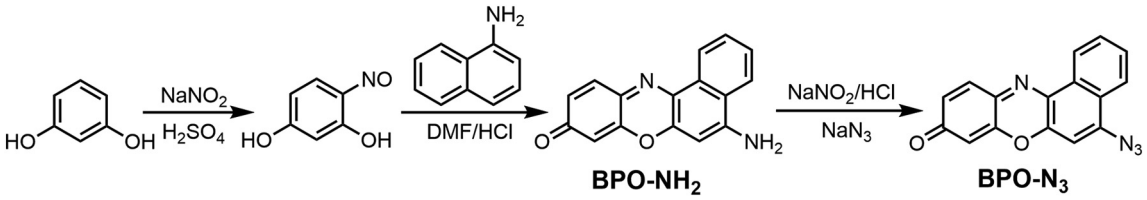

Fig. 1. Synthesis of **BPO-N_3** probe.

2.2. Synthesis of ***BPO-N_3***

The synthesis route is shown in Fig. 1.

BPO-NH_2 was synthesized according to the method described in the literature [32]. MS (*m/z*) calcd for $[C_{16}H_{11}N_2O_2]^+$: 263.0815, found: 263.0819 (Fig. S1). ^{1}H NMR (300 MHz, DMSO-d_6) δ 9.05 (d, 1H), 8.05 (dd, 2H), 7.70 (dd, 1H), 7.56 (d, 1H), 6.97 (d, 1H), 6.68 (s, 1H), 6.42 (s, 1H), 5.79 (s, 2H) (Fig. S2).

At 0 °C, $NaNO_2$ (69 mg, 1.0 mmol) was dissolved in 2 mL of water, and the solution was then mixed with 20 mL of diluted hydrochloric acid containing BPO-NH_2 (262 mg, 1.0 mmol). After stirring for 20 min, 3 mL of NaN_3 (75 mg, 1.5 mmol) aqueous solution was added, and the reaction solution was then stirred for 24 h at room temperature. The resultant crude product was filtered and recrystallized with acetonitrile, from which the probe **BPO-N_3** (220 mg, 76% yield) was obtained. MS (*m/z*) calcd for $[C_{16}H_9N_4O_2]^+$: 289.0720, found: 289.0720 (Fig. S3). ^{1}H NMR (300 MHz, DMSO-d_6) δ 8.82 (d, 1H), 8.32 (d, 1H), 8.02 (dd, 1H), 7.84 (dd, 1H), 7.67 (d, 1H), 7.36 (s, 1H), 6.94 (d, 1H), 6.39 (s, 1H) (Fig. S4). ^{13}C NMR (75 MHz, DMSO-d_6) δ 189.78, 154.26, 151.45, 151.34, 147.02, 139.96, 138.64, 135.09, 134.07, 131.54, 131.38, 127.84, 127.80, 125.78, 107.52, 104.75 (Fig. S5).

2.3. H_2S detection procedure

The stock solution of **BPO-N_3** (1 mM) was prepared by dissolving an appropriate amount of probe in DMSO. The sodium hydrosulfide solid was added to aqueous solution to prepare a H_2S solution. 4 mL of PBS buffer (50 mM, pH 7.4) was mixed with 50 μL of **BPO-N_3** (1 mM) and a certain amount of H_2S solution. The final volume of the solution was adjusted to 5 mL by ultra-pure water. The mixture was incubated at room temperature for 30 min. The absorption and emission spectra of the mixture were measured in a 1-cm quartz cuvette at an excitation wavelength of 540 nm.

2.4. Theoretical calculation

The optimal geometrical structures and electron transition of the probe were calculated by DFT/TDDFT using B3LYP/def2SVP-GD3(BJ) basis sets on Gaussian 16 software [33]. The obtained data were further analyzed by Multiwfn 3.7 software [34]. The effect of the solvent was calculated by SMD model, and water was used as the solvent in the calculation.

2.5. Cell experiment

Cell cytotoxicity: HepG2 cells were grown in DMEM liquid medium at 37 °C under 5% CO_2 atmosphere. HepG2 cells were passed and plated to ~70% confluence in 96-well plates 24 h before treatment. Then, 1 mM **BPO-N_3** stock solutions were added to obtain final concentrations of 1, 5, 10, 25, and 50 μM respectively. The treated cells were incubated for 24 h at 37 °C under 5% CO_2. Subsequently, cells were treated with 5 mg mL^{-1} MTT (40 μL $well^{-1}$) and incubated for an additional 4 h. Then the cells were dissolved in DMSO (150 μL $well^{-1}$). At last, the cell viability was measured and counted using a microplate reader.

Cell culture and imaging: HepG2 cells were grown in DMEM liquid medium at 37 °C under 5% CO_2 atmosphere. The adhered cells were incubated with 10 μM probe in an incubator for 30 min. After washing three times with PBS, the cells were further incubated with H_2S for 30 min and were then subjected to imaging. The images were captured at two emission wavelength ranges of 550–580 nm and 600–640 nm.

3. Results and discussion

3.1. Absorption spectral changes of probe in response to H_2S

The color and absorption spectrum of the probe **BPO-N_3** before and after reacting with H_2S were significantly different, as shown in Fig. 2 (A). Before adding H_2S, the color of the probe **BPO-N_3** was green, and the maximum absorption wavelength was 530 nm. Upon the addition

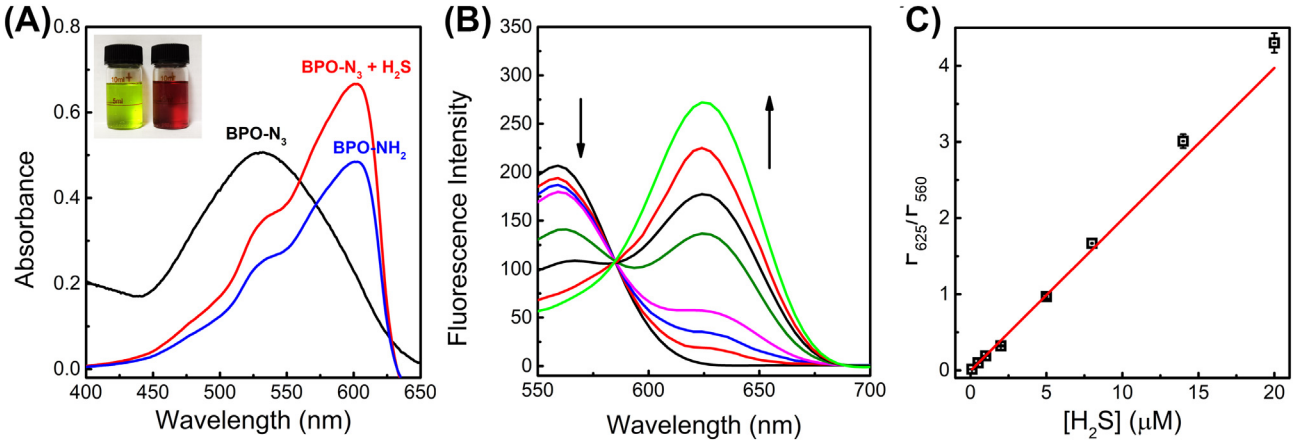

Fig. 2. (A) Absorption spectra of **BPO-N_3** (20 μM) before and after reacting with H_2S (200 μM), and of BPO-NH_2 (10 μM). Inset is the color change. (B) Fluorescence spectra of **BPO-N_3** (10 μM) in the presence of 0–20 μM H_2S. (C) Linear relationship between fluorescence intensity ratio (F_{625}/F_{560}) and concentration of H_2S (0.1–20 μM).

Table 1
Comparison of the present method with other reported H_2S selective fluorescence probe.

Probe name	Reaction medium	$\lambda_{ex}/\lambda_{em}$ (nm)	LOD (nM)	Ref.
BPO-N_3	DMSO:PBS (1:99, v/v, 50 mM, pH 7.4)	540/(625/560)	30	This work
Probe	DMF:PBS (1:9, v/v, 10 mM, pH 7.4)	510/639	36	[35]
Mito-NIR-SH	DMSO:PBS (1:99, v/v, 10 mM, pH 7.4)	670/720	89.3	[36]
1	DMSO:PBS (1:99, v/v, 20 mM, pH 7.4)	530/565	120	[37]
Probe 1	DMSO:PBS (1:3, v/v, 10 mM, pH 7.4)	395/537	220	[38]
L	DMF/HEPES (4/6, v/v, 10 mM, pH 7.4)	496/607	3390	[39]

of H_2S, the solution color was changed from green to purple, and the maximum absorption peak was shifted to 600 nm, which is consistent with the characteristic peak of BPO-NH_2.

3.2. Fluorescence spectral change of probe in response to H_2S, and linear relationship

To investigate the fluorescence spectral properties of **BPO-N_3** in response to H_2S, we first determined the change of fluorescence spectra of **BPO-N_3** after reacting with H_2S at different concentrations. Fig. 2 (B) shows the fluorescence spectra recorded at an excitation wavelength of 540 nm and an emission wavelength of 560 nm. After H_2S was added, the emission peak was red shifted to 625 nm, and with the increase of H_2S concentration, the intensity of the emission peak at 560 nm gradually decreased, while that at 625 nm gradually increased. Moreover, the absolute quantum yield after the addition of H_2S (0.22) is higher than that of **BPO-N_3** (0.19). The ratio of the emission intensity before and after the reaction (F_{625}/F_{560}) was calculated and was found to increase by about 30 times from 0.013 to 4.3. The relationship diagram (Fig. 2(C)) further showed that the intensity ratio F_{625}/F_{560} had a good linear relationship with H_2S concentrations between 0.1 and 20 μM, the equation of which was $F_{625}/F_{560} = 0.199 \times [H_2S]$-0.057, and the limit of detection (LOD) was 30 nM using the formula DL = 3σ/k. According to Table 1, the LOD of **BPO-N_3** was lower than most of the previously reported fluorescent probes.

3.3. Optimization of reaction conditions between probe and H_2S

The effects of pH, temperature and reaction time on the system were investigated in detail. As can be seen in Fig. 3(A), the probe **BPO-N_3** and its reaction product BPO-NH_2 were nearly unaffected by pH at a range of 7.0–8.0; and since the physiological pH usually is 7.4, this indicates that

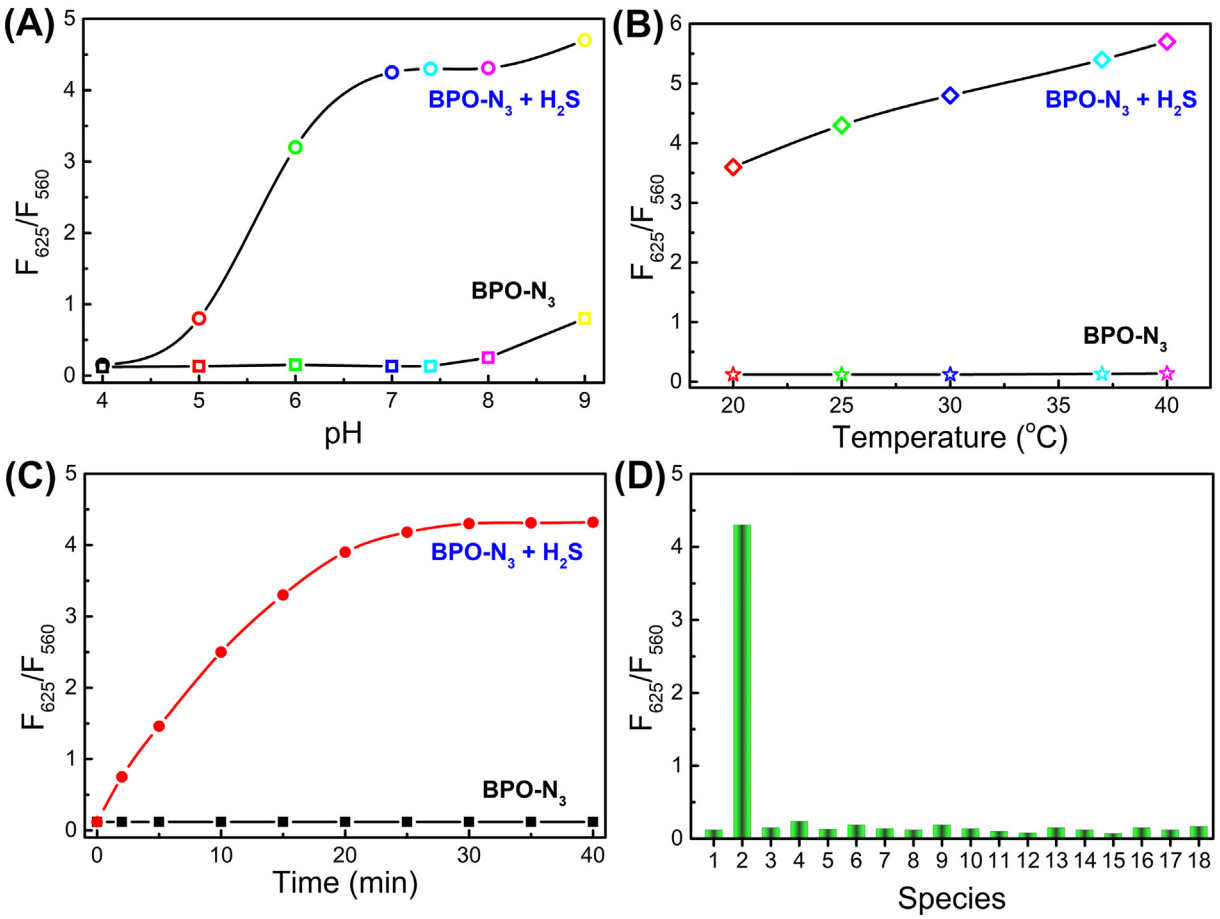

Fig. 3. Effects of reaction conditions on fluorescence intensity ratio (F_{625}/F_{560}) of **BPO-N_3** (10 μM) in the absence and presence of H_2S (20 μM). (A) Effect of pH; the reaction was performed in PBS buffer with different pH values at room temperature for 30 min. (B) Effect of reaction temperature; the reaction was performed at different temperatures in PBS buffer (pH 7.4) for 30 min. (C) Effects of time; the reaction was conducted for different lengths of time at room temperature in PBS buffer (pH 7.4). (D) Fluorescence intensity ratio (F_{625}/F_{560}) of **BPO-N_3** (10 μM) in the presence of various species: (1) only **BPO-N_3**; (2) 20 μM H_2S; (3) 100 μM Na_2SO_3; (4) 100 μM $NaHSO_3$; (5) 100 μM Na_2SO_4; (6) 100 μM $Na_2S_2O_3$; (7) 100 μM $CaCl_2$; (8) 100 μM $MgCl_2$; (9) 100 μM $ZnCl_2$; (10) 50 μM H_2O_2; (11) 50 μM HClO; (12) 50 μM $\bullet O_2^-$; (13) 50 μM •OH; (14) 100 μM $NaNO_2$; (15) 1 mM Cys; (16) 1 mM Hcy; (17) 1 mM GSH; (18) 1 mM BSA.

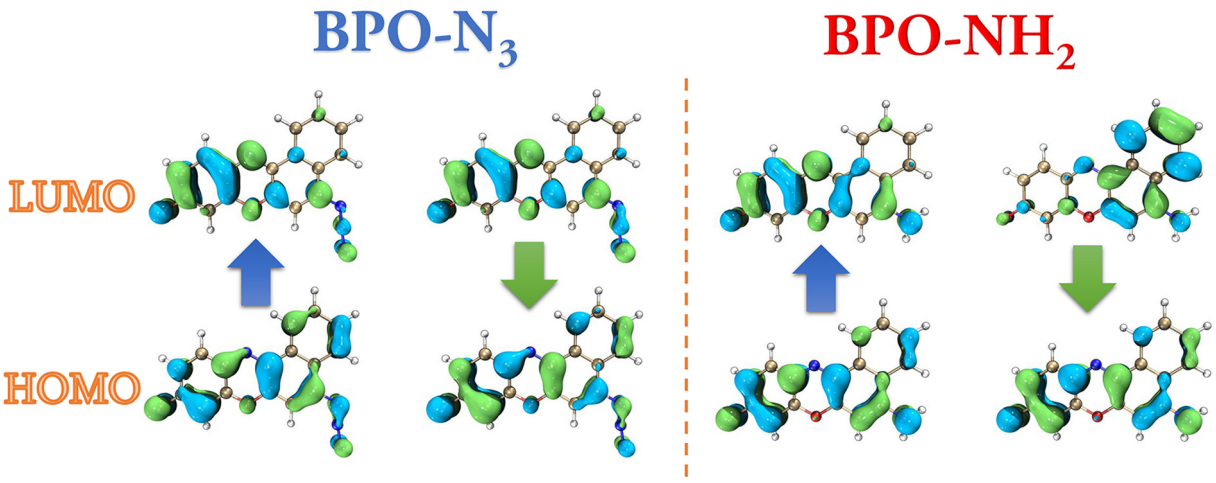

Fig. 4. Frontier molecular orbital profiles of **BPO-N_3** and BPO-NH_2 based on TDDFT (B3LYP/def2SVP-GD3(BJ)) calculations.

the probe can suitably be used in physiological environment. The experiment on the effect of temperature (Fig. 3(B)) showed that the response of the probe to H_2S increased with the increase of temperature, and the probe could effectively react with H_2S at room temperature (25 °C). Therefore, for convenience, we chose room temperature as the reaction temperature in subsequent experiments. Fig. 3(C) shows the relationship between the reaction time and the fluorescence intensity ratio, which illustrates that the reaction reached the plateau after 30 min. Finally, we concluded that the optimal reaction conditions were pH 7.4, room temperature and 30 min.

3.4. Selectivity of probe

We investigated the effects of various interference species (including inorganic salts, oxidizing species, proteins, and some sulfur-containing compounds) on the probe **BPO-N_3**. As illustrated in Fig. 3 (D), the fluorescence intensity ratio F_{625}/F_{560} of the sample in the presence of H_2S was significantly higher compared with that in the presence of other species. This indicates that probe **BPO-N_3** is more selective toward H_2S than other species. Therefore, the probe **BPO-N_3** can suitably be applied for the detection of H_2S in biological systems.

3.5. Mechanism of reaction between probe and H_2S

To study the reaction mechanism of **BPO-N_3** and H_2S, the reaction products were analyzed by ESI-MS. The mass spectrum data exhibited a molecular ion peak at $m/z = 263.0820$, which is consistent with the theoretical peak ($m/z = 263.0815$) of BPO-NH_2 (the product of a reaction between **BPO-N_3** and H_2S) in CH_3OH (Fig. S6).

In addition, we carried out TDDFT theoretical calculation to analyze the optical properties of the probe **BPO-N_3** before and after the reaction with H_2S. Fig. 4 shows the structure of the corresponding ground and excited states, and the electron cloud distribution in the corresponding molecular orbital. The calculated maximum adsorption peak of **BPO-N_3** was 525 nm (f = 0.9466), and that of BPO-NH_2 was 598 nm (f = 0.5013). The main electron transition occurred between the HOMO and the LUMO energy levels, which is similar to the experimental results, in which the spectral red shift was observed. The structure of the first excited state S_0 was optimized, and the fluorescence emission was obtained. The theoretical emission peaks of the two fluorescence emissions were 555 and 624 nm, which were the results of the transition between the LUMO→HOMO energy levels. The electron cloud caused by the transition from the azide group in the probe to amino group was observed, and the push-pull electron effect in the molecule was changed, which caused the red shift observed in the emission spectrum.

3.6. Cell imaging

HepG2 cells were selected as the model cells. Prior to cell imaging, MTT experiment was carried out to analyze the cytotoxicity of the probe. The survival rate of the cells incubated with 50 μM **BPO-N_3** was greater than 85%, indicating that the probe **BPO-N_3** has low cytotoxicity (Fig. S7). We then carried out cell imaging experiment, and the results are shown in Fig. 5. According to the results, HepG2 cells did not exhibit fluorescence signal, but upon treating with the probe **BPO-N_3**, obvious green fluorescence signal was observed. After H_2S was added to the cells, the green fluorescence signal was significantly reduced, while the red fluorescence signal was significantly enhanced. The ratio between the red and green fluorescence signals also showed that there was a significant change of color, which indicates that H_2S could instantaneously enter into the cell to react with the probe **BPO-N_3** and to generate the change of fluorescence signal. To further confirm that the fluorescence change was caused by H_2S, we pretreated HepG2 cells with $ZnCl_2$, which is an inhibitor of H_2S [13], and the results showed that there was no significant fluorescence change. Sodium nitroprusside (SNP) was further used to stimulate the production of endogenous H_2S inside the cells [31]. We first incubated the cells with SNP for 30 min before adding **BPO-N_3**. The imaging of the cells showed obvious red fluorescence, indicating that the probe could also detect endogenous H_2S. Taken together, the probe **BPO-N_3** can sensitively monitor the concentration of H_2S in living cells.

4. Conclusion

In this paper, we developed a novel probe **BPO-N_3**, using phenoxazine as the fluorescence matrix, that has high sensitivity and selectivity. The detection limit of the probe in the detection of H_2S was

Fig. 5. Confocal fluorescence imaging the H_2S in HepG-2 cells of **BPO-N_3**. (A) Only HepG-2 cells (control).(B) Only incubated with **BPO-N_3** (10 μM) for 30 min. (C–E) Incubated with the **BPO-N_3** (10 μM) for 30 min, and then incubated with 50, 100, 200 μM H_2S for 30 min. (F) Incubated with the $ZnCl_2$ (1 mM) for 1 h, and then incubated with **BPO-N_3** for 30 min, and then incubated with 100 μM H_2S for 30 min. (G) Incubated with the SNP (10 μM) for 1 h, and then incubated with **BPO-N_3** for 30 min. Excitation at 525 nm, the green channel was set at 550–580 nm, the red channel was set at 600–640 nm. Scale bar = 50 μm.

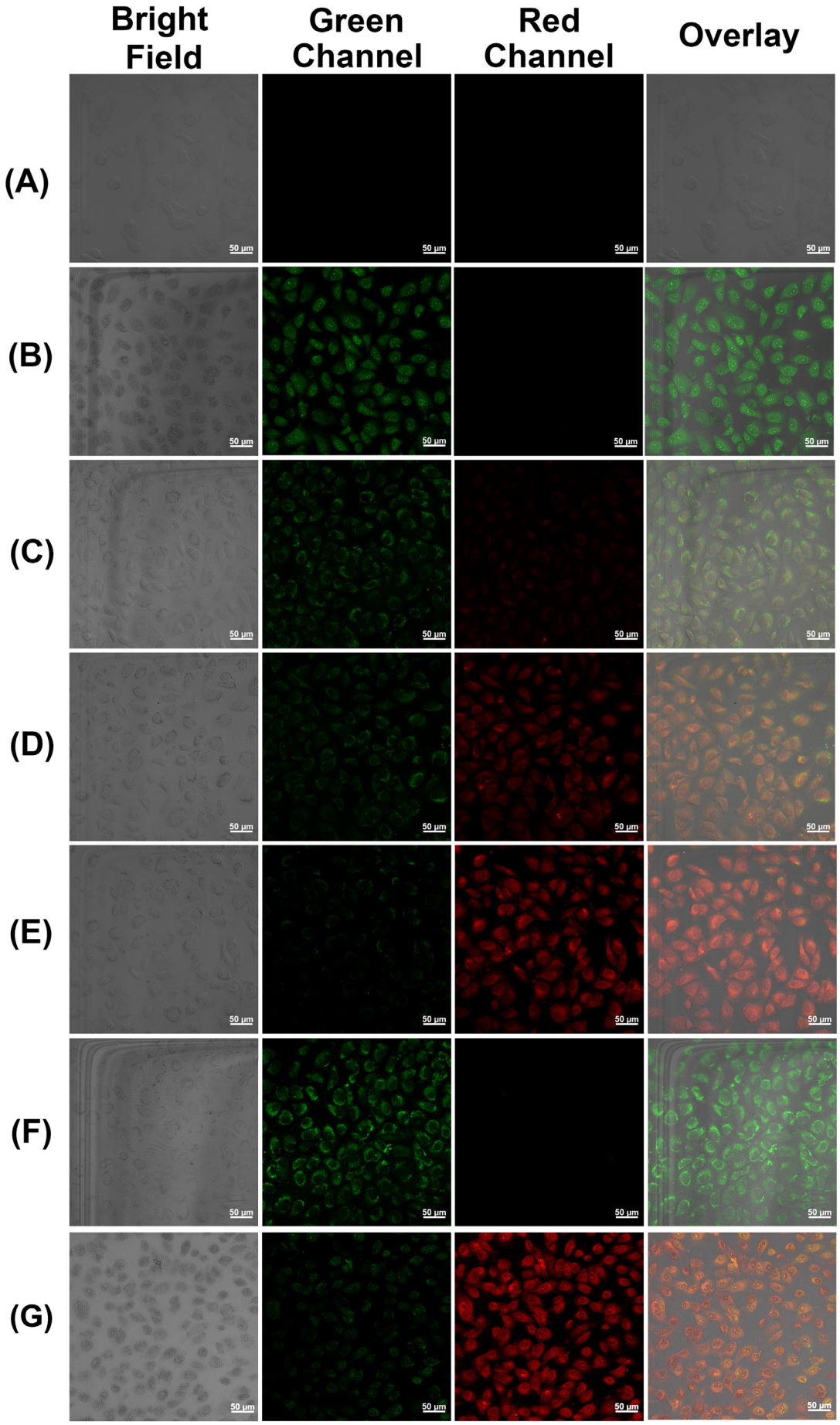
Bright Field
Green Channel
Red Channel
Overlay
(A)
(B)
(C)
(D)
(E)
(F)
(G)
50 μm

30 nM. The spectral properties of the probe were examined, the effects of pH, temperature and time on its performance were investigated, and its theoretical luminescence mechanism was calculated. Finally, the probe was successfully employed to detect exogenous and endogenous H_2S in HepG2 cells.

CRediT authorship contribution statement

Linlin Lv: Conceptualization, Methodology, Visualization, Writing - original draft. **Weiwei Luo:** Investigation, Formal analysis. **Quanping Diao:** Project administration, Funding acquisition.

Declaration of competing interest

The authors declare that they have no known competing financial interests or personal relationships that could have appeared to influence the work reported in this paper.

Acknowledgements

This work was supported by Natural Science Foundation of Liaoning Province of China (No. 2019-ZD-0358).

Appendix A. Supplementary data

Supplementary data to this article can be found online at https://doi.org/10.1016/j.saa.2020.118959.

References

[1] L. Yi, Y. Wang, T. Luo, W. Hu, M. Wang, J. Wang, Design, synthesis and evaluation of a novel hepatocyte-targeting fluorescent probe to accurately detect H_2S in mitochondria, Dyes Pigments 166 (2019) 460–466.
[2] S. Gong, E. Zhou, J. Hong, G. Feng, Nitrobenzoxadiazole ether-based near-infrared fluorescent probe with unexpected high selectivity for H_2S imaging in living cells and mice, Anal. Chem. 91 (2019) 13136–13142.
[3] Q. Zhao, J. Kang, Y. Wen, F. Huo, Y. Zhang, C. Yin, "Turn-on" fluorescent probe for detection of H_2S and its applications in bioimaging, Spectrochim. Acta Part A-Mol. Biomol. Spectrosc. 189 (2018) 8–12.
[4] Y. Zhang, L. Zhang, A novel "turn-on" fluorescent probe based on hydroxy functionalized naphthalimide as a logic platform for visual recognition of H_2S in environment and living cells, Spectrochim. Acta Part A-Mol. Biomol. Spectrosc. 235 (2020) 118331.
[5] K. Liu, C. Liu, H. Shang, M. Ren, W. Lin, A novel red light emissive two-photon fluorescent probe for hydrogen sulfide (H_2S) in nucleolus region and its application for H_2S detection in zebrafish and live mice, Sens. Actuators B-Chem. 256 (2018) 342–350.
[6] J.V. Jun, D.M. Chenoweth, E.J. Petersson, Rational design of small molecule fluorescent probes for biological applications, Org. Biomol. Chem. 18 (2020) 5747–5763.
[7] S.-H. Park, N. Kwon, J.-H. Lee, J. Yoon, I. Shin, Synthetic ratiometric fluorescent probes for detection of ions, Chem. Soc. Rev. 49 (2020) 143–179.
[8] H. Singh, K. Tiwari, R. Tiwari, S.K. Pramanik, A. Das, Small molecule as fluorescent probes for monitoring intracellular enzymatic transformations, Chem. Rev. 119 (2019) 11718–11760.
[9] Z. Zou, Z. Luo, X. Xu, S. Yang, Z. Qing, J. Liu, R. Yang, Photoactivatable fluorescent probes for spatiotemporal-controlled biosensing and imaging, TRAC-Trends Anal. Chem. 125 (2020) 115811.
[10] L. Wang, M.S. Frei, A. Salim, K. Johnsson, Small-molecule fluorescent probes for live-cell super-resolution microscopy, J. Am. Chem. Soc. 141 (2019) 2770–2781.
[11] Z. Xu, T. Qin, X. Zhou, L. Wang, B. Liu, Fluorescent probes with multiple channels for simultaneous detection of Cys, Hcy, GSH, and H_2S, TRAC-Trends Anal. Chem. 121 (2019) 115672.
[12] M. Ren, Z. Li, B. Deng, L. Wang, W. Lin, Single fluorescent probe separately and continuously visualize H_2S and HClO in Lysosomes with different fluorescence signals, Anal. Chem. 91 (2019) 2932–2938.
[13] H. Zhu, C. Liang, X. Cai, H. Zhang, C. Liu, P. Jia, Z. Li, Y. Yu, X. Zhang, W. Sheng, B. Zhu, Rational design of a targetable fluorescent probe for visualizing H_2S production under golgi stress response elicited by monensin, Anal. Chem. 92 (2020) 1883–1889.
[14] J. Sun, X. Li, J. Cao, Q. Sun, Y. Zhang, X. Wang, T. Wu, X. Hu, F. Feng, Mitochondria targeting fluorescent probes based on through bond-energy transfer for mutually imaging signaling molecules H_2S and H_2O_2, Chem. Eur. J. 25 (2019) 9164–9169.
[15] H. Zhang, X. Xia, H. Zhao, G.-N. Zhang, D.-Y. Jiang, X.-Y. Xue, J. Zhang, A near-infrared fluorescent probe based on SNAr reaction for H_2S/GSH detection in living cells and zebrafish, Dyes Pigments 163 (2019) 183–189.
[16] T. Fang, X.-D. Jiang, C. Sun, Q. Li, BODIPY-based naked-eye fluorescent on-off probe with high selectivity for H_2S based on thiolysis of dinitrophenyl ether, Sens. Actuators B-Chem. 290 (2019) 551–557.
[17] F. Qi, Y. Zhang, B. Wang, W. Chen, L. Yang, Z. Yang, X. Song, A fluorescent probe for the dicriminatory detecion of Cys/Hcy, GSH and H_2S in living cells and zebrafish, Sens. Actuators B-Chem. 296 (2019) 126533.
[18] J. Qian, D. Gong, Z. Teng, J. Wang, T. Cao, K. Iqbal, W. Liu, A. Iqbarl, W. Qin, H. Guo, 2-Vinylfuran substituted BODIPY H_2S fluorescent turn on probe based on hydrolysis of furfural and nucleophilic addition of double bond, Sens. Actuators B-Chem. 297 (2019) 126712.
[19] L. Jin, X. Tan, L. Dai, H. Bai, Q. Wang, Modulation of fluorescence sensing properties of coumarin-based fluorescent probe for H_2S and its application in cell imaging, Spectrochim. Acta Part A-Mol. Biomol. Spectrosc. 221 (2019) 117187.
[20] X. Lin, X. Lu, J. Zhou, H. Ren, X. Dong, W. Zhao, Z. Chen, Instantaneous fluorescent probe for the specific detection of H_2S, Spectrochim. Acta Part A-Mol. Biomol. Spectrosc. 213 (2019) 416–422.
[21] D. Shen, J. Liu, L. Sheng, Y. Lv, G. Wu, P. Wang, K. Du, Design, synthesis and evaluation of a novel fluorescent probe to accurately detect H_2S in hepatocytes and natural waters, Spectrochim. Acta Part A-Mol. Biomol. Spectrosc. 228 (2020) 117690.
[22] H. Niu, B. Ni, K. Chen, X. Yang, W. Cao, Y. Ye, Y. Zhao, A long-wavelength-emitting fluorescent probe for simultaneous discrimination of H_2S/Cys/GSH and its bioimaging applications, Talanta 196 (2019) 145–152.
[23] D. Andina, J.-C. Leroux, P. Luciani, Ratiometric fluorescent probes for the detection of reactive oxygen species, Chem. Eur. J. 23 (2017) 13549–13573.
[24] L. Wu, A.C. Sedgwick, X. Sun, S.D. Bull, X.-P. He, T.D. James, Reaction-based fluorescent probes for the detection and imaging of reactive oxygen, nitrogen, and sulfur species, Acc. Chem. Res. 52 (2019) 2582–2597.
[25] J.-L. Zhu, Z. Xu, Y. Yang, L. Xu, Small-molecule fluorescent probes for specific detection and imaging of chemical species inside lysosomes, Chem. Commun. 55 (2019) 6629–6671.
[26] P. Gao, W. Pan, N. Li, B. Tang, Fluorescent probes for organelle-targeted bioactive species imaging, Chem. Sci. 10 (2019) 6035–6071.
[27] Y. Zuo, X. Wang, Z. Gou, W. Lin, Step-wise functionalization of polysiloxane towards a versatile dual-response fluorescent probe and elastomer for the detection of H_2S in two-photon and NO in near-infrared modes, Chem. Commun. 56 (2020) 1121–1124.
[28] H. Zhu, C. Liu, C. Liang, B. Tian, H. Zhang, X. Zhang, W. Sheng, Y. Yu, S. Huang, B. Zhu, A new phenylsulfonamide-based Golgi-targeting fluorescent probe for H2S and its bioimaging applications in living cells and zebrafish, Chem. Commun. 56 (2020) 4086–4089.
[29] X. Song, Y. Wang, J. Ru, Y. Yang, Y. Feng, C. Cao, K. Wang, G. Zhang, W. Liu, A mitochondrial-targeted red fluorescent probe for detecting endogenous H_2S in cells with high selectivity and development of a visual paper-based sensing platform, Sens. Actuators B-Chem. 312 (2020) 127982.
[30] T. Zhou, Y. Yang, K. Zhou, M. Jin, M. Han, W. Li, C. Yin, Efficiently mitochondrial targeting fluorescent imaging of H_2S invivo based on a conjugate-lengthened cyanine NIR fluorescent probe, Sens. Actuators B-Chem. 301 (2019) 127116.
[31] X. Shi, C. Yin, Y. Wen, F. Huo, A dual-sites fluorescent probe based on symmetric structure of naphthalimide derivative to detect H_2S, Dyes Pigments 165 (2019) 38–43.
[32] L. Xu, M. Wu, L. Zhao, H. Han, S. Zhang, P. Ma, Y. Sun, X. Wang, D. Song, A novel highly sensitive and near-infrared fluorescent probe for detecting hypochlorite and its application in actual water sample and bioimaging, Talanta 215 (2020) 120892.
[33] M.J. Frisch, G.W. Trucks, H.B. Schlegel, G.E. Scuseria, M.A. Robb, J.R. Cheeseman, G. Scalmani, V. Barone, et al., Gaussian 16, Revision A.03, Gaussian Inc., Wallingford CT, 2016.
[34] T. Lu, F. Chen, Multiwfn: a multifunctional wavefunction analyzer, J. Comput. Chem. 33 (2012) 580–592.
[35] J. Wang, Y. Wen, F. Huo, C. Yin, Based 'successive' nucleophilic substitution mitochondrial-targeted H_2S red light emissive fluorescent probe and its imaging in mice, Sens. Actuators B-Chem. 297 (2019) 126773.
[36] X.-j. Zhao, Y.-t. Li, Y.-r. Jiang, B.-q. Yang, C. Liu, Z.-h. Liu, A novel "turn-on" mitochondria-targeting near-infrared fluorescent probe for H_2S detection and in living cells imaging, Talanta 197 (2019) 326–333.
[37] C. Ma, C. Wei, X. Li, X. Zheng, B. Chen, M. Wang, P. Zhang, X. Li, A mitochondria-targeted dual-reactable fluorescent probe for fast detection of H_2S in living cells, Dyes Pigments 162 (2019) 624–631.
[38] W. Luo, H. Xue, J. Ma, L. Wang, W. Liu, Molecular engineering of a colorimetric two-photon fluorescent probe for visualizing H_2S level in lysosome and tumor, Anal. Chim. Acta 1077 (2019) 273–280.
[39] K. Zhong, S. Zhou, X. Yan, X. Li, S. Hou, L. Cheng, X. Gao, Y. Li, L. Tang, A simple H_2S fluorescent probe with long wavelength emission: application in water, wine, living cells and detection of H_2S gas, Dyes Pigments 174 (2020) 108049.